

Generative multitask learning mitigates target-causing confounding

Taro Makino¹ Krzysztof Geras^{1,2} Kyunghyun Cho^{1,3,4}

Abstract

We propose a simple and scalable approach to causal representation learning for multitask learning. Our approach requires minimal modification to existing ML systems, and improves robustness to prior probability shift. The improvement comes from mitigating unobserved confounders that cause the targets, but not the input. We refer to them as target-causing confounders. These confounders induce spurious dependencies between the input and targets. This poses a problem for the conventional approach to multitask learning, due to its assumption that the targets are conditionally independent given the input. Our proposed approach takes into account the dependency between the targets in order to alleviate target-causing confounding. All that is required in addition to usual practice is to estimate the joint distribution of the targets to switch from discriminative to generative classification, and to predict all targets jointly. Our results on the Attributes of People and Taskonomy datasets reflect the conceptual improvement in robustness to prior probability shift.

1. Introduction

Deep neural networks (DNNs) excel at extracting patterns from unstructured data, but these patterns can fail to generalize outside of the training distribution. These failures are often attributed to DNNs learning spurious dependencies rather than causal relations (Ribeiro et al., 2016; Jo & Bengio, 2017; Geirhos et al., 2020). Therefore, there is a concerted effort to make patterns learned by DNNs satisfy certain properties of causal relations, such as invariance and modularity (Schölkopf, 2019; Schölkopf et al., 2021). This research direction is called causal representation learning.

Existing approaches to causal representation learning of

¹Center for Data Science, New York University ²NYU Grossman School of Medicine ³Genentech ⁴CIFAR LMB. Correspondence to: Taro Makino <taro@nyu.edu>.

Code and results are available at https://github.com/nyukat/generative_multitask_learning

ten require additional information in the form of labeled environments (Arjovsky et al., 2019; Lu et al., 2021) or labeled confounders (Puli et al., 2021). These requirements are restrictive, and therefore it is beneficial to identify more natural settings where existing information can be used for causal representation learning.

We consider the setting of multitask learning (MTL) (Caruana, 1997; Ruder, 2017; Zhang & Yang, 2017), where there is an input X and multiple targets. Without loss of generality, we consider two targets, where Y is the main target and Y' is the auxiliary target. Both targets are used for training, but predictive performance only matters for the main task. The conventional approach to MTL, which we call discriminative multitask learning (DMTL), assumes the targets are conditionally independent given the input. This implies the factorization

$$\log p(y, y' | x) = \log p(y | x) + \log p(y' | x). \quad (1)$$

During training, $\log p(y | x)$ and $\log p(y' | x)$ are estimated with separate classifiers that share a subset of their weights. Once training is complete, prediction of the main target Y is given by

$$\operatorname{argmax}_y \log p(y | x),$$

where Y' plays no role.

DMTL does not make causal assumptions explicitly, but its assumption that the targets are conditionally independent given the input is consistent with the causal graph in Fig. 1a. We argue that DMTL is flawed under two realistic causal assumptions.

First, we assume the targets cause the input, which implies we are predicting the cause from the effect. This is called anticausal learning, and is considered to encompass many common problems such as image classification (Schölkopf et al., 2012). Taking object recognition as an example, the object category can be considered to cause the pixel representation of that object.

Second, we assume there exists a variable U that causes the targets, but not the input. We call U a *target-causing confounder*. Our assumed causal graph is shown in Fig. 1b. If unobserved, U is problematic for DMTL because it induces spurious dependencies between the input and targets.

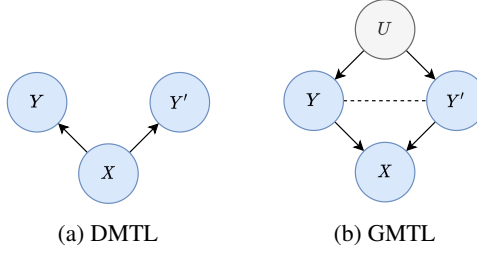


Figure 1: **(a)** The conventional approach to MTL, which we call discriminative multitask learning (DMTL), assumes the main target Y and the auxiliary target Y' are conditionally independent given the input X . DMTL is flawed under two realistic causal assumptions. **(b)** First, we assume the targets cause the input, which is called anticausal learning. Second, we assume there exists an unobserved variable U that causes the targets, but not the input. We call U a *target-causing confounder*. U induces spurious dependencies between the input and targets. This is problematic for DMTL, since it relies solely on $p(y | x)$ to predict Y , and $p(y | x)$ is affected by the spurious dependency between X and Y . Our proposed approach, which we call generative multitask learning (GMTL), mitigates target-causing confounding by conditioning on both targets. This d -separates X and U , thereby removing the spurious dependencies between the input and targets. By cutting off the influence of U , GMTL improves robustness to shifts in $p(u)$. This also improves robustness to $p(y, y')$, since U causes the targets.

The precise problem is that DMTL solely relies on $p(y | x)$ in order to predict Y , where $p(y | x)$ is influenced by the spurious dependency between X and Y . Since the spurious dependency passes through U , it makes DMTL sensitive to shifts in $p(u)$. This also makes DMTL vulnerable to shifts in $p(y, y')$, since U causes the targets. A shift in $p(y, y')$ is called prior probability shift (Storkey, 2009), and our contribution is to improve robustness to it.

Target-causing confounding can be addressed by conditioning on both targets, since this d -separates X and U , thus eliminating the spurious dependencies between the input and targets. We propose a way to achieve this by changing only the prediction method of DMTL, while keeping training the same. Keeping training the same allows us to build upon the strong foundations laid out by existing work, and is particularly beneficial since training is notoriously difficult in MTL (Standley et al., 2020).

We propose generative multitask learning (GMTL), which takes estimates of $\log p(y | x)$ and $\log p(y' | x)$ learned in the same way as DMTL, and solves

$$\operatorname{argmax}_{y, y'} \log p(x | y, y')$$

in order to predict Y . Crucially, both targets are considered

in order to predict Y . This is analogous to conditioning on both targets, which cuts off the confounding influence of U . We turn DMTL into GMTL simply by incorporating an estimate of $p(y, y')$, where Y and Y' are not assumed to be independent. Moreover, we devise a way to smoothly interpolate between the two extremes of DMTL and GMTL. This is useful if one considers the trade-off between in-distribution and o.o.d. prediction. DMTL is suitable for in-distribution prediction, since the influence of U , despite being spurious, is predictive if $p(u)$ does not change. In contrast, GMTL performs better in o.o.d. settings, specifically under prior probability shift.

We perform experiments on two datasets called Attributes of People (Bourdev et al., 2011) and Taskonomy (Zamir et al., 2018). Across various pairs of tasks on these datasets, our results show that GMTL is more robust than DMTL to prior probability shift. We attribute this improvement to GMTL’s ability to mitigate target-causing confounding. The empirical success of GMTL is evidence that causal representation learning shows promise for MTL.

2. Background

2.1. Out-of-distribution generalization

O.o.d. generalization refers to the capability of ML systems to generalize on data outside of the training distribution. Bengio et al. (2021) describe it as one of the greatest challenges in ML, and one that cannot be solved solely by scaling up datasets and computation. The failure of ML systems to generalize o.o.d. is a general problem that has been reported across a wide range of problems spanning computer vision and natural language processing (D’Amour et al., 2020). The core issue is this - when ML systems are trained to optimize an objective function, it is often easier for them to learn patterns that are dataset-specific, rather than those that hold universally. These dataset-specific patterns have many names, such as surface statistical regularities (Jo & Bengio, 2017), non-robust features (Tsipras et al., 2019), and shortcuts (Geirhos et al., 2020). We take a causal perspective and adopt the term *spurious dependencies*, which are defined as statistical dependencies not supported by causal links (Pearl, 2009).

2.2. Dataset biases induce spurious dependencies

The following example shows that spurious dependencies can arise from design choices in dataset creation. Recht et al. (2019) demonstrated that state-of-the-art image classifiers trained on ImageNet (Deng et al., 2009) failed to generalize to a replicated test set designed to mirror the original test set distribution. Engstrom et al. (2020) offered an explanation for this phenomenon. The authors reported that the dataset replication procedure relied on estimating a human-

in-the-loop metric called selection frequency, and that bias in estimating this statistic led to undesirable variation across datasets. Selection frequency is defined for an input-target pair, and measures the proportion of crowdsourced annotators who deem the pair correctly labeled. Recht et al. (2019) performed statistic matching on this metric, which corresponds to conditioning on it. Since selection frequency is caused by the input and target, this corresponds to conditioning on a collider, which induces a spurious dependency between the input and target. Such a dependency would fail to generalize o.o.d., which may explain why predictive performance degraded on the replicated test set.

In this work, we address a different source of dataset bias that we call target-causing confounding. A variable is a target-causing confounder if it is the common cause of the targets, but not the input. For a simple example, suppose we have images of people in indoor scenes, and the targets are clothing-related attributes such as hat and scarf. The season causes the targets, since people pair various types of clothing depending on the season. The season does not cause the image, since the images are of indoor scenes. Therefore, the season is a target-causing confounder that induces spurious dependencies between the input and targets. Relying on such dependencies for prediction can be problematic if the training and test sets represent different seasons.

2.3. Causal representation learning

Earlier, we made a distinction between patterns that are dataset-specific and those that hold universally. Causal inference formalizes the notion of patterns that hold universally, referring to them as causal relations (Pearl, 2009). A causal relation is a cause-effect relation modeled as a probability distribution $p(\text{effect} \mid \text{cause})$. For an example borrowed from Peters et al. (2017), consider the causal relation between altitude and temperature. Altitude causes temperature, because if we increase altitude, this generally decreases temperature. Often times, causal relations are unchanging because they are properties of nature. One of the main activities of causal inference is to estimate causal relations from data. These relations are expected to apply to all future test cases. This means that o.o.d. generalization is a basic requirement for causal models, and not merely a desirable property. However, a significant weakness of traditional causal inference is that the data must be in the form of causal variables, such as altitude and temperature. That is, it cannot handle unstructured data such as images or raw text. Since modeling unstructured data is precisely the strength of ML, there is significant interest in combining techniques from the two fields in order to take advantage of their complementary strengths (Schölkopf, 2019; Schölkopf et al., 2021).

An idea from causal inference that is particularly promising

for o.o.d. generalization in ML is an assumption called the principle of independent mechanisms (Peters et al., 2017). This assumption states that causal relations are invariant to changes in other causal relations. In order to illustrate this idea, let us again consider the relation between altitude and temperature. Let A denote temperature and T be temperature, where A causes T . The joint distribution $p(a, t)$ can be factorized in two ways,

$$p(a, t) = p(t \mid a)p(a) = p(a \mid t)p(t).$$

Now, suppose there is a shift in the marginal distribution of altitude from $p(a)$ to $q(a)$. This shifts the joint distribution to $q(a, t)$, which can again be factorized in two ways,

$$q(a, t) = q(t \mid a)q(a) = q(a \mid t)q(t).$$

The key idea from causal inference that is relevant to o.o.d. generalization in ML is that we expect

$$p(t \mid a) = q(t \mid a)$$

to hold. The reason is that $p(t \mid a)$ represents $p(\text{effect} \mid \text{cause})$, and is a causal relation. This corresponds to the mechanism of nature that causes temperature to decrease w.r.t. altitude. We do not expect this relation to change, even if $p(a)$ changes. Therefore, we expect $q(a, t)$ to factorize as

$$q(a, t) = p(t \mid a)q(a), \quad (2)$$

where $q(a) \neq p(a)$. In other words, the shift in the joint distribution can be isolated to a shift in $p(a)$. This invariance of $p(t \mid a)$ to shifts in $p(a)$ exemplifies the principle of independent mechanisms.

Conversely, we do not expect

$$p(a \mid t) = q(a \mid t)$$

to hold, since $p(a \mid t)$ represents $p(\text{cause} \mid \text{effect})$. With this non-causal factorization, when $p(a)$ shifts, both $p(a \mid t)$ and $p(t)$ must shift in a coordinated way. To summarize, with the causal factorization, the shift in the joint distribution can be isolated to a single factor. In contrast, with the non-causal factorization, the shift in the joint distribution leads to a shift in both factors.

This invariance property is extremely valuable for o.o.d. generalization. One of the main goals of causal representation learning is to learn such invariant distributions from data under weak and generic assumptions (Schölkopf et al., 2021). Our work follows this principle. We make an assumption that the targets cause the input, which implies $p(x \mid y, y')$ is a causal relation. This motivates us to switch from the discriminative distribution $p(y, y' \mid x)$ to the generative distribution $p(x \mid y, y')$. By the principle of independent mechanisms, we expect $p(x \mid y, y')$ to remain invariant when $p(y, y')$ shifts. In other words, we aim to improve robustness to prior probability shift.

2.4. Weakening the ignorability assumption

In causal inference, one often makes the assumption of ignorability, which states that there are no unobserved confounders. When ignorability fails to hold, causal relations are unidentifiable. Ignorability is a strong assumption, so it is beneficial to weaken it. For an example of existing work in this direction, Wang & Blei (2019) weakened no unobserved confounding to no unobserved single-cause confounding. Our work also belongs to this category, since we weaken ignorability by allowing unobserved target-causing confounding.

2.5. Multitask learning

MTL can reduce computational cost through parameter sharing, and improve predictive performance over training on each task individually (Standley et al., 2020). Its use is widespread, spanning domains such as scene understanding (Chowdhuri et al., 2019; Zamir et al., 2018; 2020), medical diagnosis (Kyono et al., 2021), natural language processing (McCann et al., 2018; Wang et al., 2019; Radford et al., 2019; Liu et al., 2019; Worsham & Kalita, 2020; Aghajanyan et al., 2021), recommender systems (Covington et al., 2016; Ma et al., 2018), and reinforcement learning (Kalashnikov et al., 2021).

The distinction between main and auxiliary targets is common (Ruder, 2017; Liebel & Körner, 2018; Vafaeikia et al., 2020), but not universal, and is primarily important for concerns such as which loss to use for early stopping (Caruana, 1997). We assume this distinction exists throughout this paper, denoting the main task as Y and the auxiliary task as Y' . However, our method still applies if we specify an arbitrary target to be the main target, and the others as being auxiliary.

2.6. Generative classification

Generative classification refers to learning $p(x, y)$ in order to predict Y from X (Ng & Jordan, 2001). This is in contrast to discriminative classification, where $p(y | x)$ is learned directly. Existing work has shown that generative classification in single task learning (STL) offers advantages in terms of robustness to distribution shift (Li et al., 2019; Mackowiak et al., 2021). In contrast to these works, we study the robustness of generative classification in MTL while adopting a causal perspective.

3. Generative multitask learning

The objective of GMLT is to condition on both targets in order to mitigate target-causing confounding, and improve robustness to prior probability shift. This can be done by using $\text{argmax}_{y, y'} p(x | y, y')$ for prediction, while incor-

porating the dependency between the targets. However, directly estimating $p(x|y, y')$ can be very difficult when X is high-dimensional. Additionally, it would be highly desirable to keep the training method the same as the conventional approach of DMTL, so that we can build upon extensive existing work. We can achieve this by noticing that we do not require access to a normalized probability distribution in order to query $\text{argmax}_{y, y'} p(x | y, y')$. That is, we can use Bayes rule to write

$$\begin{aligned} \text{argmax}_{y, y'} \log p(x | y, y') &= \text{argmax}_{y, y'} \log \frac{p(y, y' | x)p(x)}{p(y, y')} \\ &= \text{argmax}_{y, y'} \underbrace{\log p(y | x) + \log(y' | x)}_{\text{Eq. (1)}} - \log p(y, y'), \end{aligned} \quad (3)$$

where the marginal likelihood $p(x)$ drops out. This shows that we can turn DMTL into GMLT by additionally estimating and removing the effect of $p(y, y')$.

3.1. Removing the effect of $p(y, y')$

In order to understand what it means to remove the effect of $p(y, y')$, we consider where such dependencies come from. We imagine two cases. In the first case, there exists a common *cause* U that gives rise to both Y and Y' , or

$$p(y, y') = \int p(y|u)p(y'|u)p(u)du.$$

U is called a confounder, since it induces a statistical dependency between Y and Y' that is not a causal relation.

In the other case, there exists a common *effect* U that is caused by the target variables. U is called a collider, and conditioning on it induces a dependency between Y and Y' due to the explaining-away phenomenon. This case corresponds to when we know some variables that are caused by the target variables, just like the input X , but are not in our interest to take into account for the problem of classification.

In both of these cases, the existence of an extra variable U , either unobserved or observed, leads to a *spurious* dependency between the targets. GMLT in Eq. (3) removes this spurious dependency via the $\log p(y, y')$ term. This in turn removes the spurious dependencies between the input and targets that pass through U .

3.2. Mitigating target-causing confounding

We are particularly interested in the first case of having an unobserved confounder U . Consider the setting of STL, where Y' does not exist, and we learn the relation between X and Y in isolation. If U is unobserved, it unblocks the path $Y \leftarrow U \rightarrow X$. This is called a backdoor path, and induces a spurious dependency between X and Y . This spurious dependency is inevitably captured by the STL classifier, which can reduce robustness. In DMTL, even though

Y and Y' are both used for training, assuming the targets are conditionally independent given the input results in a similar effect. The problem is the sole reliance on $p(y | x)$ in order to predict Y .

GMTL explicitly addresses this issue by taking into account the dependency between Y and Y' . In other words, we are demonstrating that MTL, when done in a generative manner, protects us from the issue of spurious dependency arising from a particular type of unobserved confounding that we call target-causing confounding.

3.3. Estimation of $p(y, y')$

GMTL requires estimating $p(y, y')$, which is trivial for categorical targets. The maximum likelihood estimate of $p(y, y')$ is obtained by counting the number of occurrences of the pair (y, y') , and dividing by the total across all pairs. However, there is an important precaution to be made, since it is possible that certain pairs of (y, y') are never observed. This is problematic, since $p(y, y') = 0$ results in taking a logarithm of zero in Eq. 3. This can be addressed with additive smoothing, where a pseudocount $\epsilon > 0$ is added to the count for each pair prior to normalization.

3.4. Interpolation between discriminative and generative classification

We have proposed a method for removing the spurious dependencies between the input and targets that are induced by the target-causing confounder U . While this spurious dependency may fail to generalize outside of the training distribution, it can help predictive performance when training and test distributions are similar. In other words, there is often a trade-off between predictive performance in i.i.d. and o.o.d. settings, as previously reported in Tsipras et al. (2019). We therefore introduce a multiplicative factor $\alpha \in [0, 1]$ which allows us to interpolate between discriminative and generative classification. We define our prediction function as

$$\operatorname{argmax}_{y, y'} \log p(y, y' | x) - \alpha \log p(y, y').$$

This corresponds to DMTL for $\alpha = 0$, and GMTL when $\alpha \in (0, 1]$. Increasing α decreases the degree to which we rely on spurious dependencies induced by target-causing confounders for prediction.

4. An illustrative example

Here, we construct a synthetic example where a target-causing confounder U induces a spurious dependency between X and Y . We illustrate how DMTL is sensitive to this dependency, while GMTL is invariant to it.

Suppose there are two targets $Y, Y' \in \{0, 1\}$ that cause

the input $X \in \mathbb{R}$. Let us assume that $p(y, y')$ is bivariate Bernoulli with parameters p, p' and $\sigma_{Y, Y'}$, where $p(y = 1) = p$, $p(y' = 1) = p'$, and $\operatorname{Cov}(Y, Y') = \sigma_{Y, Y'}$. Let us assume X is generated by a mixture of Gaussians with latent variable $2Y + Y'$, or

$$\begin{aligned} p(x | y = 0, y' = 0) &= \mathcal{N}(x; 0, \sigma_0^2), \\ p(x | y = 0, y' = 1) &= \mathcal{N}(x; 1, \sigma_1^2), \\ p(x | y = 1, y' = 0) &= \mathcal{N}(x; 2, \sigma_2^2), \\ p(x | y = 1, y' = 1) &= \mathcal{N}(x; 3, \sigma_3^2). \end{aligned}$$

The value of $\sigma_{Y, Y'}$ is set by an unobserved variable U . U is a target-causing confounder, since it causes Y and Y' , but not X . The data generating process follows the graph in Fig. 1b. We fix $p = p' = 0.5$, $\sigma_0^2 = \sigma_1^2 = 0.4$, and $\sigma_2^2 = \sigma_3^2 = 0.6$, and interpolate $\sigma_{Y, Y'}$ from -0.2 to 0.2. In other words, the only property of the data generating process that changes is the prior dependency between Y and Y' .

Fig. 2 shows how the decision boundaries of DMTL and GMTL with $\alpha = 1$ are affected by changes in $\sigma_{Y, Y'}$. The decision boundary of DMTL is the value of x for which the solution to $\operatorname{argmax}_y p(y | x)$ changes, where Y' has been marginalized out. In contrast, the decision boundary of GMTL is the value of x where the Y portion of the solution to $\operatorname{argmax}_{y, y'} p(x | y, y')$ changes. The decision boundary for DMTL changes in response to $\sigma_{Y, Y'}$, while it remains constant for GMTL. This is because GMTL with $\alpha = 1$ only uses the Gaussian densities for prediction, which have no connection to $\sigma_{Y, Y'}$.

In this example, we have shown that GMTL and DMTL arrive at different solutions by changing only the dependency between Y and Y' induced by the target-causing confounder U . The key difference between the two methods is that DMTL uses the spurious dependency between X and Y , while GMTL does not. Which of the two methods achieves better predictive performance depends on the particular test distribution, since the spurious dependency will be useful in i.i.d. settings, and not in o.o.d. settings.

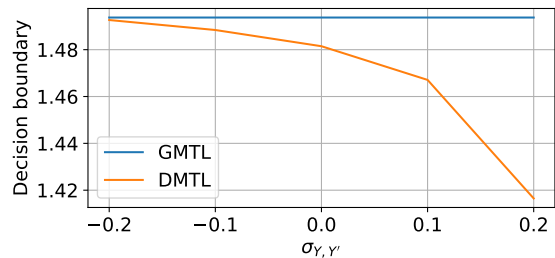


Figure 2: Here we show how the decision boundaries of GMTL and DMTL change w.r.t. $\sigma_{Y, Y'}$. DMTL is sensitive to changes in $\sigma_{Y, Y'}$, while GMTL is invariant.

5. Experimental setup

In our experiments, we compare GMTL and DMTL in terms of robustness to prior probability shift across two datasets, multiple pairs of classification tasks, and two MTL methods. Here we describe our experimental setup.

5.1. Datasets and tasks

Attributes of People. The Attributes of People dataset (Bourdev et al., 2011) consists of 8,035 images of people. There are 4,013 examples in the training set, and 4,022 in the test set. Since the authors did not specify a validation set, we use 20% of the training set as the validation set. Each image comes labeled with up to nine binary attributes: male, long hair, glasses, hat, t-shirt, long sleeves, shorts, jeans, and long pants. We use each attribute as a binary classification task and predict whether the attribute appears in the image. We drop the gender attribute, since it has the potential for negative downstream applications (Wang & Kosinski, 2018). We experiment with various pairs of tasks, taking turns specifying one as the main task, and the other as the auxiliary task. For each pair of tasks, we report the classification accuracy for the main task. Since not all attributes are labeled for each example, we consider the three pairs of tasks with the highest number of co-occurrences. These are: hat and long sleeves, long hair and hat, and glasses and hat.

Taskonomy. The Taskonomy dataset (Zamir et al., 2018) is of a much larger scale than the first dataset, containing approximately four million images of indoor scenes. We use a subset of the dataset that is provided by the authors for faster experimentation, with 548,785 examples in the training set, 121,974 in the validation set, and 90,658 in the test set. Each image comes paired with twenty six labels relevant to scene understanding, but since we are focusing on classification, we only use the object and scene annotations as targets. We use the object annotations as a 100-way object classification task, and the scene annotations as a 64-way scene classification task. Between object and scene classification, we take turns specifying one as the main task, and the other as the auxiliary task. We report the top-1 accuracy for the main task.

5.2. MTL methods

No Parameter Sharing (NPS). The first MTL method we use is a trivial combination of the two trained STL networks. We call this No Parameter Sharing (NPS). This is equivalent to STL networks during training, but becomes different during prediction if $\alpha > 0$, since the STL networks influence one another through the $-\alpha \log p(y, y')$ term. While NPS is primarily meant to be a simple setting for comparing GMTL and DMTL, it offers some practical

utility as well. MTL methods are notoriously difficult to train, and it is often challenging to get them to perform better than the STL baseline (Alonso & Plank, 2017). NPS combined with GMTL offers a way to combine two STL networks to reap the benefits of MTL simply by estimating $p(y, y')$ and predicting jointly over Y and Y' .

Cross-stitch Networks (CSN). For the second MTL method, we use a soft-parameter sharing method called Cross-stitch Networks (CSN) (Misra et al., 2016). CSN is also relatively simple. It takes two trained STL networks, and takes a linear combination of the activations at each layer during the forward pass. Training CSN involves learning the coefficients of the linear combinations, as well as fine-tuning the STL network weights.

5.3. Methodology for training and prediction

For all datasets and tasks, we use ResNet-50 (He et al., 2016) pretrained on ImageNet (Deng et al., 2009) for the STL networks. We train using Adam (Kingma & Ba, 2015) with L_2 regularization. We tune the learning rate and regularization multiplier. For data augmentation, during training we resize the images to 256×256 , randomly crop them to 224×224 and randomly horizontally flip them. During validation and testing, we resize the images to 256×256 , and center crop them to 224×224 . For all experiments, we train STL networks from five random initializations.

5.4. Simulating prior probability shift with importance sampling

The purpose of these experiments is to compare GMTL and DMTL under prior probability shifts of varying severity. Since it is impractical to collect many different test sets, we simulate prior probability shifts using importance sampling. Suppose that the original test distribution is

$$p(x, y, y') = p(x | y, y')p(y, y'),$$

and the simulated test distribution is

$$q(x, y, y') = q(x | y, y')q(y, y').$$

Based on our assumption that the targets cause the input, $p(x | y, y')$ is a causal relation. Additionally, by the principle of independent mechanisms, we assume

$$p(x | y, y') = q(x | y, y'). \quad (4)$$

In other words, the simulated test distribution can be written

$$q(x, y, y') = p(x | y, y')q(y, y'), \quad (5)$$

and the shift in the joint distribution can be isolated to a shift in $p(y, y')$. This means that the expected loss $l(x, y, y')$

under the simulated test distribution $q(x, y, y')$ is given by

$$\begin{aligned} \mathbb{E}_{q(x, y, y')}[l(x, y, y')] &= \mathbb{E}_{p(x|y, y')q(y, y')}[l(x, y, y')] \\ &= \mathbb{E}_{p(x, y, y')} \left[\frac{q(y, y')}{p(y, y')} l(x, y, y') \right] \\ &\approx \frac{1}{N} \sum_{n=1}^N \frac{q(y^{(n)}, y'^{(n)})}{p(y^{(n)}, y'^{(n)})} l(x^{(n)}, y^{(n)}, y'^{(n)}) \\ &\approx \sum_{n=1}^N \omega^{(n)} l(x^{(n)}, y^{(n)}, y'^{(n)}), \end{aligned}$$

where

$$\omega^{(n)} = \frac{q(y^{(n)}, y'^{(n)})}{p(y^{(n)}, y'^{(n)})} \Big/ \sum_{m=1}^N \frac{q(y^{(m)}, y'^{(m)})}{p(y^{(m)}, y'^{(m)})}.$$

We can now compute the accuracy under various o.o.d. $q(y, y')$'s and visualize how the accuracy changes w.r.t. the distance between $p(y, y')$ and $q(y, y')$.

5.5. Measuring the severity of distribution shift between $p(y, y')$ and $q(y, y')$

We need a metric to measure the severity of distribution shift between $p(y, y')$ and $q(y, y')$, such that predictive performance degrades w.r.t. the severity of shift. Not all metrics satisfy this criteria. To build intuition, consider a single task binary classification problem where $P(Y = 1) = \theta$. If we use a norm-based metric such as total variation, this treats a change in θ from 0.6 to 0.8 and a change from 0.6 to 0.4 as being the same. However, from the point of view of prediction, the latter should be more detrimental, since it reverses the ranking of the classes.

Similarly, Kullback-Leibler (KL) divergence is a common choice for measuring the distance between distributions, but it suffers from a related problem. Consider θ changing from 0.9 to 0.9999, and from 0.9 to 0.4. Due to taking the logarithm of a small number, KL divergence considers the first to be a more severe shift. This is undesirable, because the change from 0.9 to 0.4 represents a reversal in the ranking of the classes.

These examples point to a need for a ranking-based metric, since a significant change to the ranking of classes is detrimental to predictive performance. Weighted rank correlation satisfies this. If the weighted rank correlation between $p(y, y')$ and $q(y, y')$ is positive with large magnitude, it means that there are no significant changes in the ranking of classes, and that the distribution shift is not severe. In contrast, if the weighted rank correlation is negative with large magnitude, it implies the rankings of classes has changed significantly. This constitutes a more severe distribution shift. We therefore use weighted Kendall's τ (Shieh, 1998), which we henceforth refer to as τ , to measure the severity of

distribution shift between $p(y, y')$ and $q(y, y')$. We provide the definition of τ in the supplementary material. It relies on a weighting function, for which we use $1/(r + 1)$, where r is the ranking.

5.6. Sampling $q(y, y')$

Our choice of metric informs how to sample $q(y, y')$, since our goal is to evaluate across a wide range of distribution shift severities. We designed a method which shuffles $\log p(y, y')$ and perturbs it with noise. To be precise, let $f(y, y') \in \{1, 2, \dots, |\mathcal{Y} \times \mathcal{Y}'|\}$ such that each (y, y') is assigned a unique integer index. We use $p_{f(y, y')} = p(y, y')$. Let $i = \alpha \cdot |\mathcal{Y} \times \mathcal{Y}'|$, where $\alpha \sim \mathcal{U}(0, 0.5)$. We randomly shuffle these indices with $\pi : \{1, 2, \dots, i\} \rightarrow \{1, 2, \dots, \alpha \times i\}$. then, we define $q(y, y')$ by

$$q(y, y') \propto \begin{cases} \exp(\log p(y, y') + \epsilon) & \text{if } f(y, y') > i \\ \exp(\log p_{\pi(f(y, y'))} + \epsilon) & \text{if } f(y, y') \leq i, \end{cases}$$

where $\epsilon \sim \mathcal{N}(0, \sigma^2)$ and $\sigma \sim \mathcal{U}(10^{-12}, 5)$.

6. Results

We compare the robustness of GML ($\alpha \in (0, 1]$) and DML ($\alpha = 0$) to prior probability shift. We repeat the following procedure. First, we simulate an o.o.d. test set by sampling $q(y, y')$, and compute τ . τ represents the severity of distribution shift between $q(y, y')$ and the original test distribution $p(y, y')$. We then use importance sampling to compute the o.o.d. accuracy under $q(y, y')$ for a range of α .

The results are split into five groups that are equally spaced in terms of τ . Each group represents the accuracies for a range of α under a particular severity of distribution shift. For each group, we compute the value of α that attains the highest accuracy. Since these are test set results, this optimal α can be thought of as given to us by an oracle. We also compute the difference in accuracy between GML and DML at the optimal value of α for each group.

We observe strikingly similar results for both datasets and all pairs of tasks. As the distribution shift becomes more severe, the optimal α increases. A representative example for each dataset is shown in the left subfigures in Fig. 3, and the rest are in the supplementary material. This matches our expectations - increasing α removes more of the spurious dependencies induced by target-causing confounders, which is more beneficial for severe distribution shifts.

Also, as the severity of distribution shift increases, the difference in accuracy between GML and DML for the optimal α increases as well. This can be seen in the right subfigures in Fig. 3, and is also in-line with our expectations. As the distribution shift becomes more severe, the spurious dependencies induced by target-causing confounding become

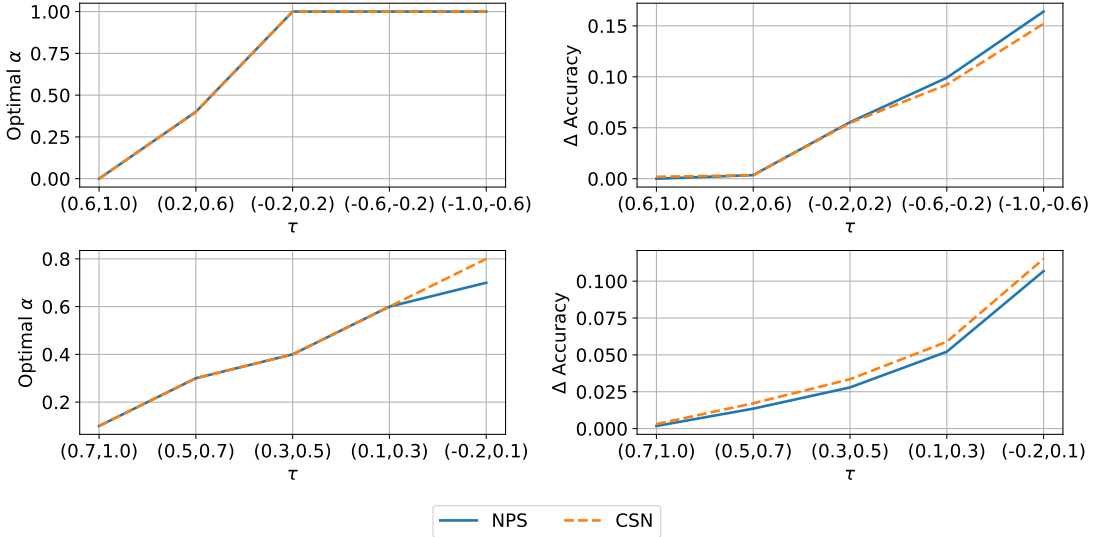


Figure 3: **Comparing the robustness of GMTL and DMTL to prior probability shift.** We compute the o.o.d. accuracy across a range of α values, where $\alpha \in [0, 1]$ is GMTL, and $\alpha = 0$ is DMTL. The results are grouped w.r.t. the severity of distribution shift τ , and we report the optimal α for each group. As seen in the left subfigures, as the distribution shift becomes more severe from left to right, the optimal α monotonically increases for both Attributes of People (top left) and Taskonomy (bottom left). This is because larger α removes more spurious dependencies induced by target-causing confounding, which is more beneficial when the shift severity increases. In the right subfigures, the vertical axis is the difference in accuracy between GMTL and DMTL. The gain in accuracy from using GMTL increases w.r.t. the severity of distribution shift for both Attributes of People (top right) and Taskonomy (bottom right). The reason is that the spurious dependencies induced by target-causing confounding become less predictive as the shift severity increases, and therefore removing them yields larger improvements in accuracy. These patterns hold very similarly for NPS and CSN, meaning that it is our formulation of GMTL, rather than the particular parameterization of $p(y, y' | x)$, that drive these improvements.

less predictive, and removing them yields larger gains in robustness.

Both patterns hold very similarly for NPS and CSN. This suggests that it is our formulation of GMTL that yields these improvements, rather than the particular parameterization used to learn $p(y, y' | x)$. We start with MTL networks that perform strongly w.r.t. their respective STL baselines, as seen in Tables 1 and 2, and significantly improve robustness to prior probability shift through our generative reformulation of MTL.

Table 1: Test set accuracy for hat and long sleeves in the Attributes of People. MTL outperforms the STL baseline, which is a basic requirement for MTL.

	Hat	Long sleeves
STL	0.917 ± 0.003	0.853 ± 0.004
MTL	0.920 ± 0.001	0.861 ± 0.005

In summary, both the optimal α , as well as the corresponding gain in accuracy using GMTL, increase monotonically w.r.t. the severity of distribution shift. This is a strong re-

Table 2: Top-1 test set accuracy for object and scene classification on Taskonomy. MTL outperforms the STL baseline.

	Object	Scene
STL	0.749 ± 0.001	0.730 ± 0.001
MTL	0.750 ± 0.001	0.737 ± 0.001

lation that holds across datasets, pairs of tasks, and MTL methods. To quantify the generality of this result, we aggregate all of our results, and compute the correlation between τ and the optimal α . Since τ is used in the context of an interval, we take the midpoint of each interval. This results in a correlation of -0.847. This indicates a strong positive correlation between the severity of distribution shift and the optimal α . The generality of this relation is strong evidence that our formulation of GMTL improves robustness to target-causing confounding.

7. Conclusion

We presented generative multitask learning (GMTL), which is an approach for causal representation learning for MTL

that requires minimal changes to existing ML systems. Our approach mitigates the effect of target-causing confounders, which are variables that cause the targets, but not the input. This removes spurious dependencies between the input and targets, thereby improving robustness to prior probability shift.

We incorporated a parameter α to control the degree to which spurious dependencies induced by target-causing confounding are used for prediction. This allows GMTL to manage the trade-off between i.i.d. and o.o.d. predictive performance. The optimal value of α , as well as the gain in accuracy from using GMTL, both tend to increase w.r.t. the severity of distribution shift in $p(y, y')$. This relation holds consistently across datasets, pairs of tasks, and MTL methods. This is strong evidence that our generative formulation of MTL improves robustness to target-causing confounding.

In presenting our results, we assumed oracle access to the optimal α . A limitation of GMTL is that in practice, the optimal α depends on factors that cannot be determined in advance, such as the severity of distribution shift that will be encountered, and whether the shift is static or dynamic. Unknown factors such as these prevent us from giving a generic problem-agnostic procedure for selecting α . Problem-specific procedures to select α require future study.

Another limitation of GMTL is that it requires estimating the target joint distribution without making independence assumptions. This can quickly become difficult as the number of tasks grows.

Looking forward, we are excited by the new perspectives that causal representation learning can bring to existing ML paradigms. Our work demonstrates the potential for this in the context of MTL. We plan to investigate what other areas of ML can be improved by adopting a causal perspective.

8. Acknowledgements

This work was supported in part by grants from the National Institutes of Health (P41EB017183 and R21CA225175), the National Science Foundation (HDR-1922658), the Gordon and Betty Moore Foundation (9683), and Samsung Advanced Institute of Technology (under the project *Next Generation Deep Learning: From Pattern Recognition to AI*).

References

Aghajanyan, A., Gupta, A., Shrivastava, A., Chen, X., Zettlemoyer, L., and Gupta, S. Muppet: Massive multi-task representations with pre-finetuning. In *EMNLP*, 2021.

Alonso, H. M. and Plank, B. When is multitask learning effective? semantic sequence prediction under varying data conditions. In *EACL*, 2017.

Arjovsky, M., Bottou, L., Gulrajani, I., and Lopez-Paz, D. Invariant risk minimization. *arXiv*, abs/1907.02893, 2019.

Bengio, Y., LeCun, Y., and Hinton, G. E. Deep learning for AI. *Commun. ACM*, 64(7):58–65, 2021.

Bourdev, L. D., Maji, S., and Malik, J. Describing people: A poselet-based approach to attribute classification. In *ICCV*, 2011.

Caruana, R. *Multitask learning*. PhD thesis, Carnegie Mellon University, 1997.

Chowdhuri, S., Pankaj, T., and Zipser, K. Multinet: Multi-modal multi-task learning for autonomous driving. In *WACV*, 2019.

Covington, P., Adams, J., and Sargin, E. Deep neural networks for youtube recommendations. In *RecSys*, 2016.

D’Amour, A., Heller, K. A., Moldovan, D., Adlam, B., Alipanahi, B., Beutel, A., Chen, C., Deaton, J., Eisenstein, J., Hoffman, M. D., Hormozdiari, F., Housby, N., Hou, S., Jerfel, G., Karthikesalingam, A., Lucic, M., Ma, Y., McLean, C. Y., Mincu, D., Mitani, A., Montanari, A., Nado, Z., Natarajan, V., Nielson, C., Osborne, T. F., Raman, R., Ramasamy, K., Sayres, R., Schrouff, J., Seneviratne, M., Sequeira, S., Suresh, H., Veitch, V., Vladmyrov, M., Wang, X., Webster, K., Yadlowsky, S., Yun, T., Zhai, X., and Sculley, D. Underspecification presents challenges for credibility in modern machine learning. *arXiv*, abs/2011.03395, 2020.

Deng, J., Dong, W., Socher, R., Li, L., Li, K., and Li, F. Imagenet: A large-scale hierarchical image database. In *CVPR*, 2009.

Engstrom, L., Ilyas, A., Santurkar, S., Tsipras, D., Steinhardt, J., and Madry, A. Identifying statistical bias in dataset replication. In *ICML*, 2020.

Geirhos, R., Jacobsen, J., Michaelis, C., Zemel, R. S., Brendel, W., Bethge, M., and Wichmann, F. A. Shortcut learning in deep neural networks. *Nat. Mach. Intell.*, 2(11):665–673, 2020.

He, K., Zhang, X., Ren, S., and Sun, J. Deep residual learning for image recognition. In *CVPR*, 2016.

Jo, J. and Bengio, Y. Measuring the tendency of cnns to learn surface statistical regularities. *arXiv*, abs/1711.11561, 2017.

Kalashnikov, D., Varley, J., Chebotar, Y., Swanson, B., Jonschkowski, R., Finn, C., Levine, S., and Hausman, K. Mt-opt: Continuous multi-task robotic reinforcement learning at scale. *arXiv*, abs/2104.08212, 2021.

Kingma, D. P. and Ba, J. Adam: A method for stochastic optimization. In *ICLR*, 2015.

Kyono, T., Gilbert, F. J., and Schaar, M. V. D. Triage of 2d mammographic images using multi-view multi-task convolutional neural networks. *ACM Transactions on Computing for Healthcare*, 2(3):1–24, 2021.

Li, Y., Bradshaw, J., and Sharma, Y. Are generative classifiers more robust to adversarial attacks? In *ICML*, 2019.

Liebel, L. and Körner, M. Auxiliary tasks in multi-task learning. *arXiv*, abs/1805.06334, 2018.

Liu, X., He, P., Chen, W., and Gao, J. Multi-task deep neural networks for natural language understanding. In *ACL*, 2019.

Lu, C., Wu, Y., Hernández-Lobato, J. M., and Schölkopf, B. Nonlinear invariant risk minimization: A causal approach. *arXiv*, abs/2102.12353, 2021.

Ma, J., Zhao, Z., Yi, X., Chen, J., Hong, L., and Chi, E. H. Modeling task relationships in multi-task learning with multi-gate mixture-of-experts. In *KDD*, 2018.

Mackowiak, R., Ardizzone, L., Köthe, U., and Rother, C. Generative classifiers as a basis for trustworthy image classification. In *CVPR*, 2021.

McCann, B., Keskar, N. S., Xiong, C., and Socher, R. The natural language decathlon: Multitask learning as question answering. *arXiv*, abs/1806.08730, 2018.

Misra, I., Shrivastava, A., Gupta, A., and Hebert, M. Cross-stitch networks for multi-task learning. In *CVPR*, 2016.

Ng, A. Y. and Jordan, M. I. On discriminative vs. generative classifiers: A comparison of logistic regression and naive bayes. In *NIPS*, 2001.

Pearl, J. *Causality*. Cambridge university press, 2009.

Peters, J., Janzing, D., and Schölkopf, B. *Elements of causal inference: foundations and learning algorithms*. The MIT Press, 2017.

Puli, A. M., Zhang, L. H., Oermann, E. K., and Ranganath, R. Predictive modeling in the presence of nuisance-induced spurious correlations. *arXiv*, abs/2107.00520, 2021.

Radford, A., Wu, J., Child, R., Luan, D., Amodei, D., and Sutskever, I. Language models are unsupervised multitask learners. 2019.

Recht, B., Roelofs, R., Schmidt, L., and Shankar, V. Do imagenet classifiers generalize to imagenet? In *ICML*, 2019.

Ribeiro, M. T., Singh, S., and Guestrin, C. "why should I trust you?": Explaining the predictions of any classifier. In *SIGKDD*, 2016.

Ruder, S. An overview of multi-task learning in deep neural networks. *arXiv*, abs/1706.05098, 2017.

Schölkopf, B. Causality for machine learning. *arXiv*, abs/1911.10500, 2019.

Schölkopf, B., Janzing, D., Peters, J., Sgouritsa, E., Zhang, K., and Mooij, J. M. On causal and anticausal learning. In *ICML*, 2012.

Schölkopf, B., Locatello, F., Bauer, S., Ke, N. R., Kalchbrenner, N., Goyal, A., and Bengio, Y. Towards causal representation learning. *arXiv*, abs/2102.11107, 2021.

Shieh, G. S. A weighted kendall's tau statistic. *Statistics & probability letters*, 39(1):17–24, 1998.

Standley, T., Zamir, A. R., Chen, D., Guibas, L. J., Malik, J., and Savarese, S. Which tasks should be learned together in multi-task learning? In *ICML*, 2020.

Storkey, A. When training and test sets are different: characterizing learning transfer. *Dataset shift in machine learning*, 30:3–28, 2009.

Tsipras, D., Santurkar, S., Engstrom, L., Turner, A., and Madry, A. Robustness may be at odds with accuracy. In *ICLR*, 2019.

Vafaeikia, P., Namdar, K., and Khalvati, F. A brief review of deep multi-task learning and auxiliary task learning. *arXiv*, abs/2007.01126, 2020.

Wang, A., Singh, A., Michael, J., Hill, F., Levy, O., and Bowman, S. R. GLUE: A multi-task benchmark and analysis platform for natural language understanding. In *ICLR*, 2019.

Wang, Y. and Blei, D. M. The blessings of multiple causes. *Journal of the American Statistical Association*, 114(528): 1574–1596, 2019.

Wang, Y. and Kosinski, M. Deep neural networks are more accurate than humans at detecting sexual orientation from facial images. *Journal of personality and social psychology*, 114(2):246, 2018.

Worsham, J. and Kalita, J. Multi-task learning for natural language processing in the 2020s: where are we going? *Pattern Recognition Letters*, 136:120–126, 2020.

Zamir, A. R., Sax, A., Shen, W. B., Guibas, L. J., Malik, J., and Savarese, S. Taskonomy: Disentangling task transfer learning. In *CVPR*, 2018.

Zamir, A. R., Sax, A., Cheerla, N., Suri, R., Cao, Z., Malik, J., and Guibas, L. J. Robust learning through cross-task consistency. In *CVPR*, 2020.

Zhang, Y. and Yang, Q. A survey on multi-task learning. *arXiv*, abs/1707.08114, 2017.

A. Supplementary material

A.1. Weighted Kendall's τ

Weighted Kendall's τ (Shieh, 1998) is a measure of rank correlation between two vectors \mathbf{x} and \mathbf{y} , both with length N . Using the authors' notation, let (i, R_i) for $i = 1, \dots, N$ be pairs such that R_i is the rank of the element in \mathbf{y} whose corresponding \mathbf{x} value has rank i . Let $w(i, j)$ be a bounded and symmetric weight function that maps to \mathbb{R} , and denote its value at (i, j) as w_{ij} . Weighted Kendall's τ is defined as

$$\tau = 1 / \left(\sum_{i,j} w_{ij} - \sum_i w_{ii} \right) \sum_{i \neq j} \text{sgn}(i - j) \text{sgn}(R_i - R_j),$$

where

$$\text{sgn}(x) = \begin{cases} -1 & \text{if } x < 0 \\ 0 & \text{if } x = 0 \\ 1 & \text{if } x > 0. \end{cases}$$

A.2. Additional results

Tables 3 and 4 show that MTL performs better than or equal to the STL baseline on the remaining pairs of tasks on the Attributes of People.

Table 3: Test set accuracy for long hair and hat on the Attributes of People.

	Long hair	Hat
STL	0.858 ± 0.003	0.917 ± 0.003
MTL	0.860 ± 0.002	0.917 ± 0.002

Table 4: Test set accuracy for glasses and hat on the Attributes of People.

	Glasses	Hat
STL	0.843 ± 0.011	0.917 ± 0.003
MTL	0.848 ± 0.001	0.917 ± 0.002

Fig. 4 shows the comparison between GMTL and DMTL under prior probability shift for the same pair of tasks as Fig. 3 in the main text, but with the main and auxiliary tasks reversed. Fig. 5–8 show these results for the remaining pairs of tasks in the Attributes of People. Similar to Fig. 4, Fig. 9 shows the results for Taskonomy, but with the main and auxiliary tasks reversed in relation to the main text.

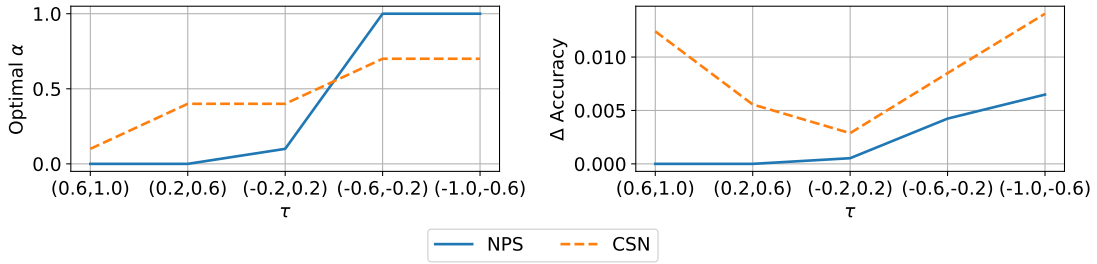


Figure 4: Attributes of people with long sleeves as the main task, and hat as the auxiliary task.

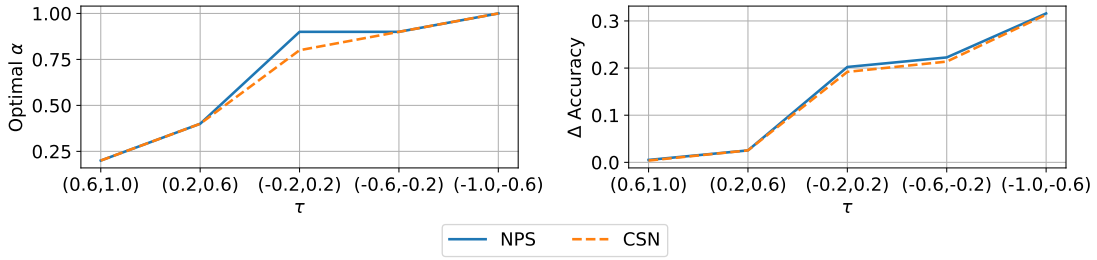


Figure 5: Attributes of people with long hair as the main task, and hat as the auxiliary task.

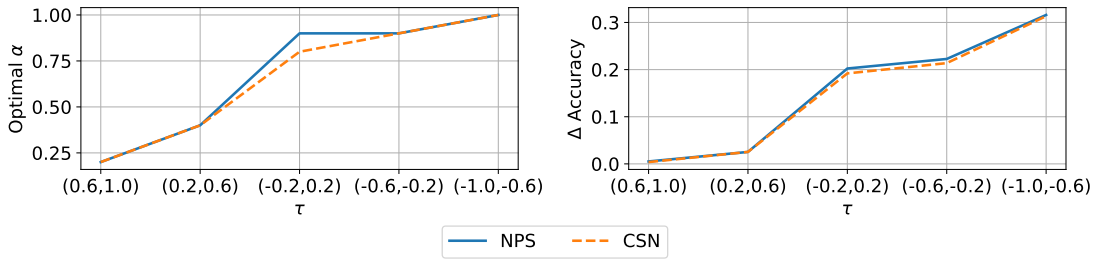


Figure 6: Attributes of people with hat as the main task, and long hair as the auxiliary task.

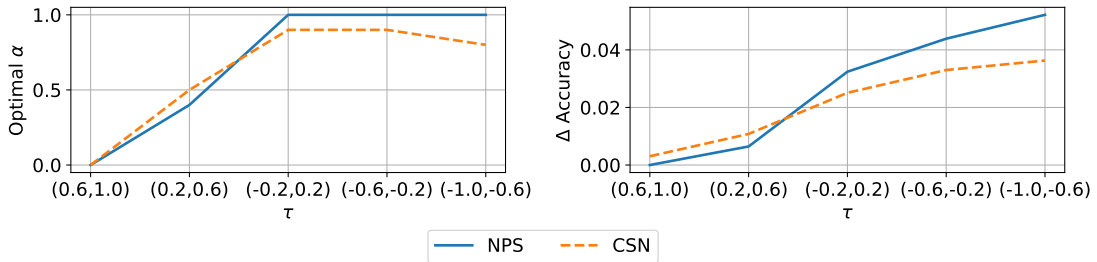


Figure 7: Attributes of people with glasses as the main task, and hat as the auxiliary task.

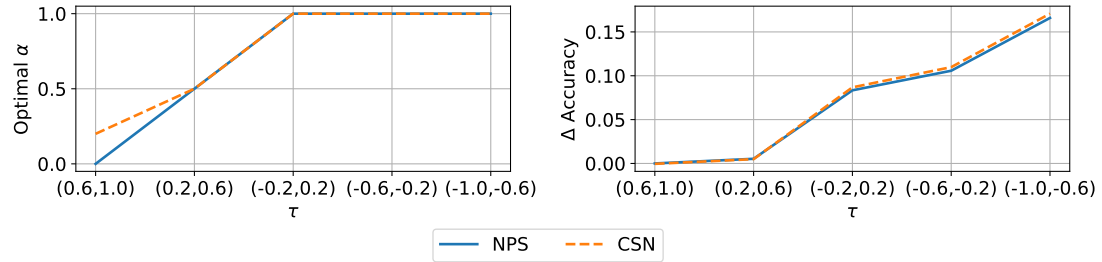


Figure 8: Attributes of people with hat as the main task, and glasses as the auxiliary task.

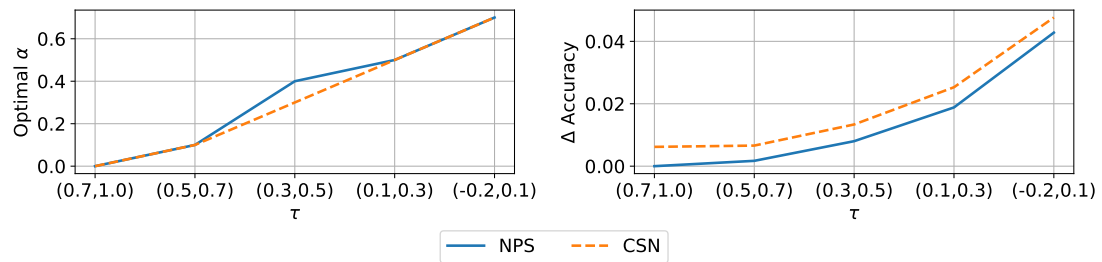


Figure 9: Taskonomy with object classification as the main task, and scene classification as the auxiliary task.